Chemical Engineering Journal 156 (2010) 226–233

Contents lists available at ScienceDirect

Chemical Engineering Journal

journal homepage: www.elsevier.com/locate/cej

Effects of mixing, seeding, material of baffles and final temperature on solution crystallization of L-glutamic acid in an oscillatory baffled crystallizer

Xiongwei Ni*, Anting Liao

Centre for Oscillatory Baffled Reactor Applications (COBRA), School of Engineering and Physical Science, Heriot-Watt University, Edinburgh EH14 4AS, UK

ARTICLE INFO

Article history:
Received 25 August 2009
Received in revised form 14 October 2009
Accepted 16 October 2009

Keywords:
Solution crystallization
Linear cooling rate
Seeding
Oscillatory baffled crystallizer
Meta-stable zone width
L-Glutamic acid

ABSTRACT

In this paper, we report the effects of mixing intensity, seeding, composition of baffle material and final temperature on meta-stable zone width (MSZW) and crystal polymorph in solution crystallization of an industrially important compound, L-glutamic acid, in an oscillatory baffled crystallizer (OBC). The results show that the MSZW decreases with increasing of mixing; meta-stable α crystals are transformed into stable β crystals with enhanced mixing intensity. Seeding meta-stable α crystals in operational conditions that promote β crystals leads to the formation of α crystals allowing co-existence of both forms; while seeding stable β crystals in conditions that favour α form allow β crystals prevailing in all conditions. Smoother surface of baffle material in OBC exhibits larger MSZW and favours meta-stable crystals, while rougher surface has smaller MSZW with stable crystals dominating. The meta-stable crystals gradually change into the stable form when final cooling temperature is closer to its nucleation temperature. The outcomes from this work indicate that by controlling process parameters desirable crystal polymorph can be obtained in the OBC.

1. Introduction

Solution crystallization is a relatively simple process; however, the underlying science is not well understood and industrial operation still heavily relies upon operators' experience. Fig. 1 is a schematic diagram describing a solution crystallization process. When a hot and under-saturated solution is cooled, it crosses the solubility curve as shown in Fig. 1 and becomes supersaturated. From a scientific viewpoint, supersaturated solutions exhibit a meta-stable zone that provides an allowable level of supersaturation for each crystallization process. In other words, until a certain degree of supersaturation has been reached (via further cooling in this case), spontaneous nucleation is not likely to occur within the meta-stable zone. Crystal growth takes place with further cooling, while the concentration of the solution decreases. The main cooling cycle must be within the meta-stable zone. It should be noted that in order to obtain desirable crystal specification, industrial-scale batch crystallization operations have to follow the "crystallization path" of the bold arrow shown in Fig. 1.

While solubility of a compound in a solution can be determined experimentally, the super-solubility (Fig. 1) or the meta-stable limit is thermodynamically not found and kinetically not well defined, depending on temperature, rate of generating supersaturation, solution history, impurities, fluid dynamics, scale, etc. [1]. This means that the super-solubility curve in Fig. 1 changes when reactor's mixing/operation/process conditions vary and when scale up of laboratory to industrial operation is involved. This is partially why it is very difficult to mimic laboratory crystallizations onto industrial-scale batch operations involving stirred tank crystallizer (STC), the workhorse of industrial crystallization.

The added complication is that our ability and understanding in scaling up STC is limited. Moreover there is no agreement on a set of parameters to be kept constant in scale up, e.g. tip impellor velocity [2], rotational speed of impellor [3,4], stirred tank Reynolds number [5], power input [4,6], ratio of impellor to vessel diameters [7], volume-averaged shear rate [8], mass transfer coefficient [9,10], mean droplet size [11], gas hold-up [12], mixing time [13] and computational dynamic simulation [14] have all been used as the scale up parameter in STC. This further worsens the controllability of industrial crystallizations in STC.

On the heat transfer side, while linear cooling profile is routinely used in laboratories, it is still impossible to be implemented in any industrial batch STC due to the fact is that the specific surface area per volume ($m^2\ m^{-3}$) for heat transfer in STC decreases dramatically with scale.

From fluid mechanic perspective, while good mixing can be attained in lab scales, mixing gradients are often found in large scale operations, with better mixing at and near the impeller regimes, poorer elsewhere [15–17]. This leads to the fact is that mixing cannot linearly be scaled up. In terms of crystallization

* Corresponding author. Tel.: +44 131 4513781; fax: +44 131 4513129.
E-mail address: x.ni@hw.ac.uk (X. Ni).

1385-8947/$ – see front matter © 2009 Elsevier B.V. All rights reserved.
doi:10.1016/j.cej.2009.10.045

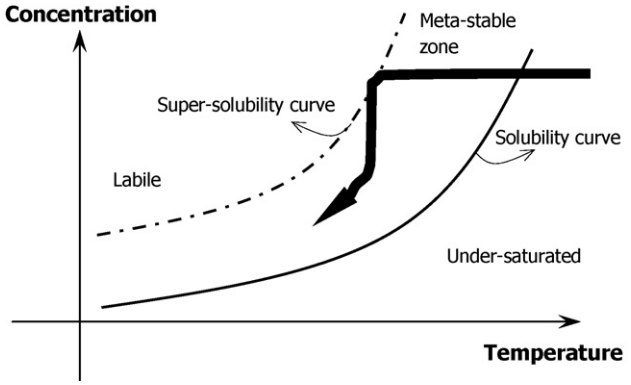

Fig. 1. General schematic of a typical solution crystallization process.

process, mixing gradients cause concentration gradients that have direct impact on crystallization science, e.g. supersaturation and meta-stable zone width. Clearly, a crystallizer with linear scale up capability, excellent heat transfer characteristics and uniform mixing would be desirable, alleviating/eliminating the aforementioned scientific and operational problems in crystallization involving STC and allowing benefits realized in laboratories to be directly applied to industrial crystallizations. The work reported in this paper is the continuation of our investigation on the suitability of oscillatory baffled crystallizer (OBC) in solution crystallization due to its linear scale up capability [18,19]. L-Glutamic acid was the model crystal compound used in this work of research. Previously we reported the effect of solution concentration and cooling rate on crystallization parameters [20], in this paper the effects of mixing, seeding, material and final temperature on solution crystallization of L-glutamic acid are presented.

The OBC consists of a column containing periodically spaced orifice baffles superimposed with oscillatory motion. Mixing in an OBC is provided by the generation and cessation of eddies when flow interacts with baffles. With repeating cycles of vortices, strong radial motions are created, giving uniform mixing in each inter-baffle zone and cumulatively along the length of the column. The fluid mechanical conditions in an OBC are governed by two dimensionless groups, namely, the oscillatory Reynolds number (Re_o) and the Strouhal number (St), defined as

$$Re_o = \frac{2\pi f x_o \rho D}{\mu} \quad (1)$$

$$St = \frac{D}{4\pi x_o} \quad (2)$$

where D is the column diameter (m), ρ the fluid density (kg m^{-3}), μ the fluid viscosity (kg m^{-1} s^{-1}), x_o the oscillation amplitude (m) and f the oscillation frequency (Hz). The oscillatory Reynolds number describes the intensity of mixing applied to the column, while the Strouhal number is the ratio of column diameter to stroke length, measuring the effective eddy propagation [21].

2. Experimental set-up and procedures

2.1. The oscillatory baffled crystallizer

Fig. 2 shows a schematic set-up of the oscillatory baffled crystallizer (OBC). The OBC was made of a jacketed glass column of 0.05 m internal diameter and 0.5 m tall, making a total volume of 1 L. The OBC was flanged onto a metal frame with a supporting structure in order to minimize external mechanical vibrations. The OBC was operated in batch mode at atmospheric pressure and room temperature. The jacket inlet and outlet were connected to a temperature controlled water bath (Techne RB-12A, UK). An inbuilt

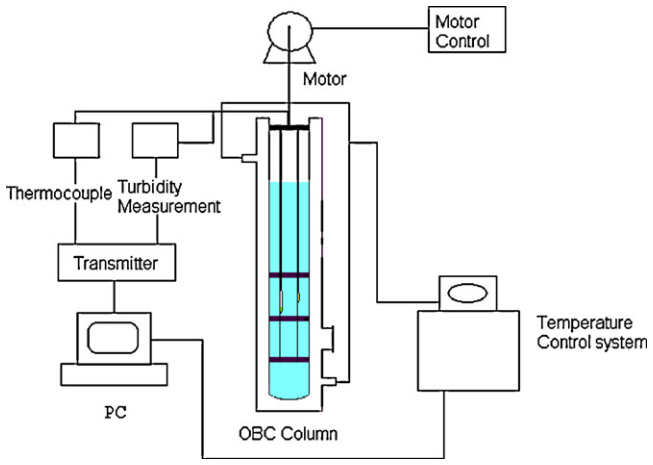

Fig. 2. The schematic of the experimental set-up (not drawn to scale).

pump ensures a steady flow of water through the jacket of the crystallizer. The water bath was controlled through an external computer.

A set of three equally spaced orifice baffles was used to generate mixing in the OBC, and supported by two 5 mm diameter PTFE rods. The baffle set was oscillated by an electrical motor/gearbox unit (Leroy Somer Ltd.) with an inverter for speed control (Eurotherm Drives 601). Oscillation frequencies of 0.2–10 Hz can be obtained by varying the rotational speed of the motor; and peak-to-peak oscillation amplitudes of 1–40 mm by adjusting the eccentric position of a connecting rod in a stainless steel coupling wheel.

2.2. Meta-stable zone width

Meta-stable zone width (MSZW) is a nucleation kinetic limited parameter that is highly dependent on process conditions [22–28]. In this work, the MSZW is determined by turbidity measurement using a fibre optic probe designed and built in-house. The turbidity measurement is based on a principle that solution transmittance is inversely proportional to concentration of crystals within the solution [29]. The details of procedures of calibration and operation can be found elsewhere [20].

Fig. 3 is a typical profile of solution transmittance as a function of temperature obtained in the OBC. Initially the signals of transmittance are low (the square symbols), indicating crystals are not yet dissolved in the solution. When the temperature increases over a certain point, a sharp rise in transmittance is seen, where the circled "points" are generally referred as the start of dissolution. As the dissolution of crystals further intensifies with increasing tem-

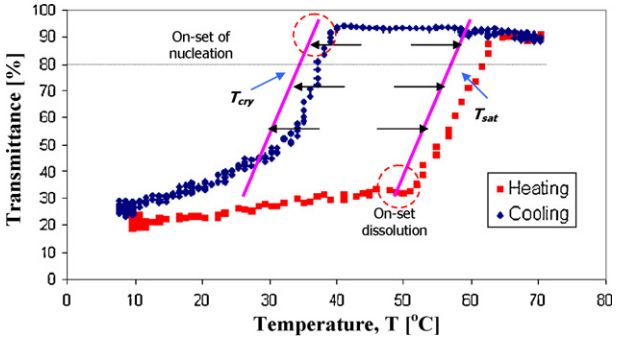

Fig. 3. A typical profile of solution transmittance as a function of temperature in crystallization of L-glutamic acid in OBC (concentration = 30 g L^{-1}, cooling rate = 0.5 °C min^{-1}).

Table 1
Properties of L-glutamic acid.

Molecular formula	Molecule weight	Density ($kg\,m^{-3}$)	Isoelectric point (pH)
$C_5H_9NO_4$	147.13	1.538	3.22

perature, a maximum transmittance signal is recorded, suggesting a clear solution free of solid.

By controlling the decrease of solution temperature, a controlled cooling, i.e. a linear cooling profile, is created, and a sharp drop in transmittance is noticed. The nucleation is initiated in a small region where the signal starts to fall; and crystallization takes place when the transmittance readings have dropped to a pre-defined value (e.g. 20% in this study, see the dotted line in Fig. 3) from the maximum [30]. The meta-stable zone width (ΔT_{max}) for a particular operational condition is then defined as

$$\Delta T_{max} = T_{sat} - T_{cry} \quad (3)$$

where T_{sat} is the saturation temperature (°C) and T_{cry} the crystallization temperature (°C) as shown in Fig. 3. It is clear that the MSZW is dependent on operational conditions.

2.3. L-Glutamic acid

L-Glutamic acid (β form 99% CAS 5686-2, EEC 200-293-7) was purchased from Sigma–Aldrich Co. Ltd. in the form of white powders and the physical properties of L-glutamic acid are given in Table 1. L-Glutamic acid crystals have two polymorphic forms: meta-stable α and stable β forms. The former has a distinctive prismatic morphology, which is easy to filter, generally preferred for industrial purposes, whereas the latter is of needle-like form, which is difficult to filter and generally requires further process steps before usage. The solubility of α L-glutamic acid crystals is higher than that of β form at any given temperature [31], as shown in Fig. 4.

2.4. Experimental procedures

A known amount of L-glutamic acid was dissolved in 1-L distilled water to give a specific solution concentration. The solution was heated up and kept at 10 °C above its saturation temperature for about 30 min in order to ensure complete dissolution of the solute material. For each solution concentration and given experimental condition, the corresponding supersaturation for alpha and beta crystals can be calculated according to Sakata's equations [31]. The solution was cooled to a final temperature of 10 °C and held for 10 min. Crystals were then filtered, washed using a 95% ethanol solution and dried in an oven at 80 °C overnight. The dry crystals were used for the analysis of crystal polymorphism using scanning electron microscope (SEM). Three samples for each condition were selected for this purpose, the numbers of α and β crystals within each frame were counted and averaged over the sample numbers using a computer software. This provides some indication on which polymorph was dominating at a corresponding experimental condition. These information are then used in the subsequent sections and discussions. For limited samples, X-ray diffraction (XRD) technique was also employed to verify crystal polymorph. Crystal size distribution was determined using Malvern Master Sizer (Malvern Instrument Ltd.), but for α crystals only. In addition, 10% of the total experiments under each operating condition were repeated for repeatability, from which the experimental error on turbidity measurement, hence MSZW data was found around about 11%.

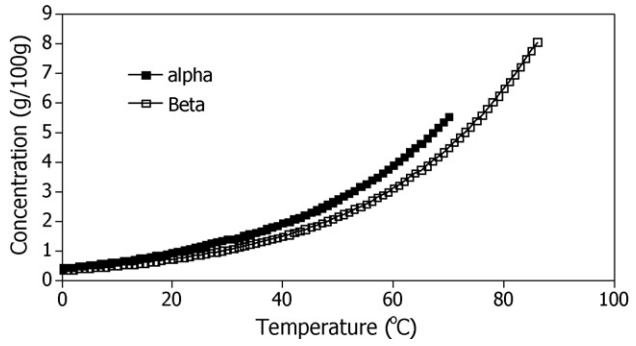

Fig. 4. Solubility curves for α and β forms of L-glutamic acid in water (Sakata [31]).

3. Results and discussions

3.1. Effect of mixing intensity on nucleation kinetics

There are generally two stages in the formation of crystals: nucleation and growth. The nucleation involves the formation of new crystals in a crystallizing environment [32], and is further divided into primary and secondary nucleation. The primary homogeneous and heterogeneous nucleation processes have very fast kinetics, often too fast to control in a reliable manner. Taking Fig. 3 as an example, when the turbidity probe registered noticeable changes in the transmittance during cooling, the nucleation process has in fact come and gone, i.e. the probe can only detect post-nucleation events. The secondary nucleation by definition occurs only in the presence of a stable parent crystal [33,34], and can be initiated through either attrition or seeding, although there are other different nucleation mechanisms. The mechanism of attrition is due to fluid dynamic induced collision between a crystal and another crystal or between a crystal and any other solid object, e.g. the walls, impellers and baffles of a crystallizer, leading to fresh nuclei being produced [35].

The crystal growth consists of layer-by-layer addition of solute to the nuclei and can be either mass transfer controlled or surface integration controlled process [32,34,36]. For mass transfer controlled solution crystallization, one of the mechanisms of transporting the solution to crystal surfaces and then taking part in surface crystallization process is by turbulent mixing [37]. Consequently, the state of mixing in a given crystallizer is an important factor in controlling the uniformity of crystal sizes as well as serving to keep crystals in suspension throughout the process. In addition, local supersaturation levels and consequent crystallizer performance are very sensitive to mixing conditions, particularly when the supersaturation generation is fast and the vessel size is large. Under local high supersaturation conditions, spontaneous nucleation occurs that lead to fine crystals with poor filtration properties. Good mixing helps even distribution of supersaturation within a given vessel and avoids spontaneous and excessive nucleation [38].

The effect of mixing intensities on crystallization of L-glutamic acid in the OBC was examined using various oscillation intensities covering the oscillation frequencies of 1–3 Hz and oscillation amplitudes of 15, 20 and 30 mm at two linear cooling rates of 0.5 and 2.0 °C min^{-1} and two concentrations of 30 and 35 g L^{-1}, totalling 36 experiments. Fig. 5 shows the MSZW against the oscillatory Reynolds numbers for the two cooling rates and concentrations; and the MSZW data from our previously studies [20,39]. It is clear that the MSZW decreased with the increase of oscillation intensity for both concentrations and cooling rates. This is expected [32] that a solution with increased mixing intensity is close to its solubility curve, hence it has a reduced MSZW. It can also be seen that at the same solution concentration, the larger the cooling rate, the wider the MSZW. This is within our expectation, as faster cooling rate creates a higher supersaturation rate within the same time scale

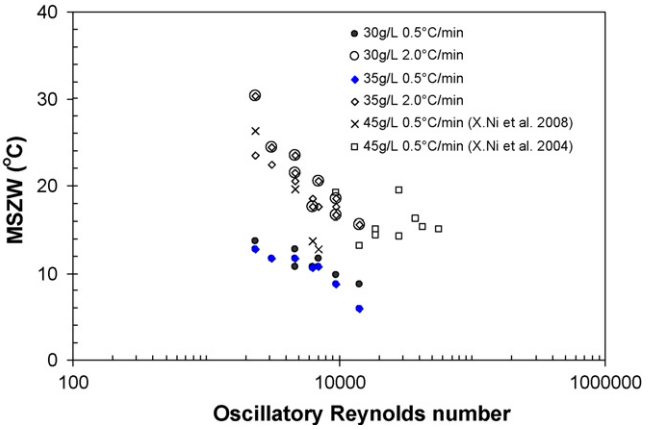

Fig. 5. Meta-stable zone width vs. oscillation Reynolds number.

[40], longer relaxation time is required to achieve a quasi-steady state distribution of molecular clusters and allow the appearance of the first nuclei cluster even at the same concentration. Hence the MSZW becomes wider, and acts effectively as a barrier for crystallization [32]. In addition, the MSZW changed little for the two concentrations at a fixed cooling rate, which agrees with the previous study [26].

The MSZW data from our previous studies are also compiled into Fig. 5. At similar mixing conditions, the slope of decrease in MSZW at 45 g L^{-1} (symbol ×) [20] is steeper than that at 30 and 35 g L^{-1} (symbols ◯ and ◊), while at much higher oscillation intensities [39], the changes in MSZW are less (symbol □). It should be noted that at the solution concentration of 45 g L^{-1}, β crystals were exclusively obtained. In contrast, the predominant polymorph at solution concentrations of 30 and 35 g L^{-1} was α.

3.2. Effect of mixing intensity on polymorphism

Fig. 6 shows the selection of SEM crystal images obtained at 35 g L^{-1} and at a cooling rate of 0.5 °C min^{-1}. At this cooling rate, α-crystals were seen at lower oscillation conditions (the top left hand corner), and transferred to β-type with the increase of oscillation frequency (the vertical dotted line) at a fixed amplitude, as well as with the increase of oscillation amplitude (the horizontal dotted line) at a fixed oscillation frequency. Using X-ray diffraction (XRD) with intensities of characteristic peaks of 4.84 Å for α and 4.14 Å for β, the percentages of β crystals were determined and seen to increase from 10.85% to 42.43% for increased oscillation intensities (see Fig. 6). This validates the qualitative SEM observations. At a higher cooling rate of 2.0 °C min^{-1}, α to β transformation was less with more α crystals appearing. It should be noted that the transformation is common for this type of crystal. Kitamura [41] reported that α L-glutamic crystal tended to nucleate and grow in stagnant bottom region of a STC, which relates to less mixed area with lower mixing intensity. The SEM photos suggest that mixing plays an important role in controlling crystal polymorph, with the higher the oscillation intensity, the more the β-crystals.

Fig. 7 is the corresponding SEM image arrays for the concentration of 30 g L^{-1} at 0.5 °C min^{-1}. The transformation from α to β was much less and α crystals dominated at this and 2.0 °C cooling rates.

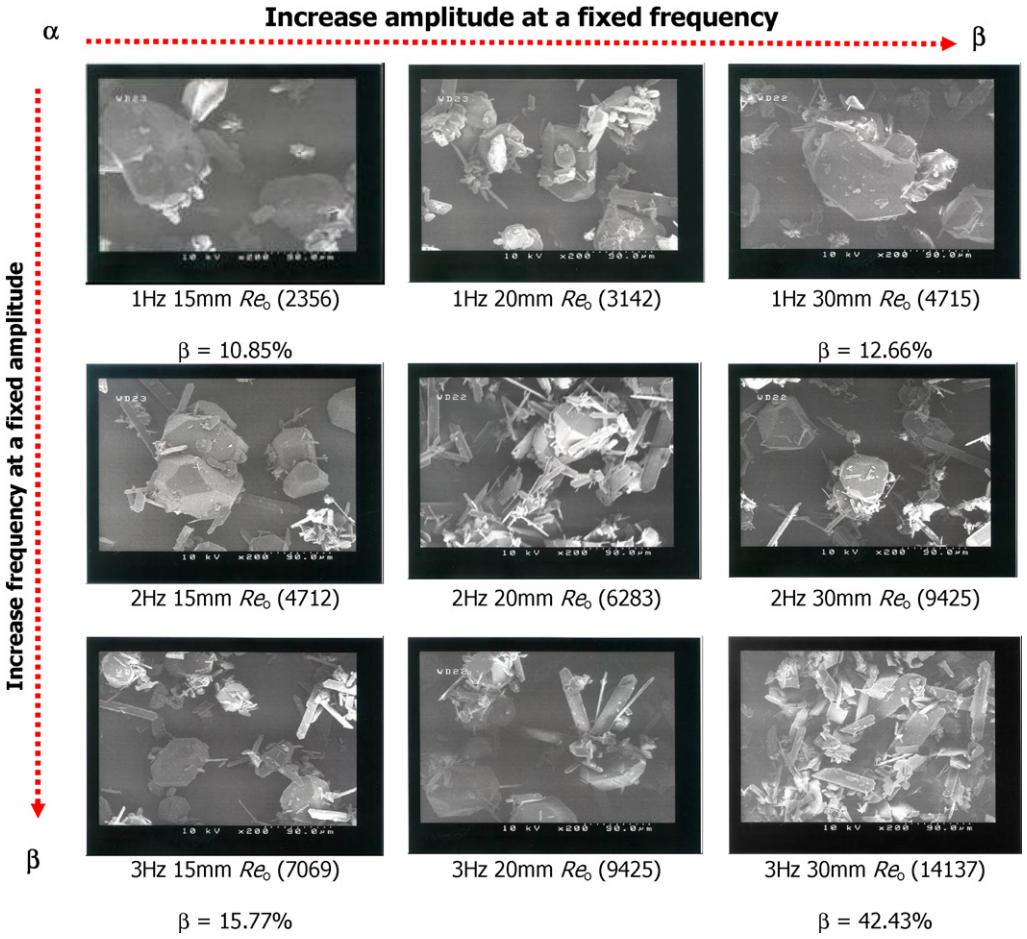

Fig. 6. SEM images crystals (cooling rate = 0.5 °C min^{-1}, conc. = 35 g L^{-1}).

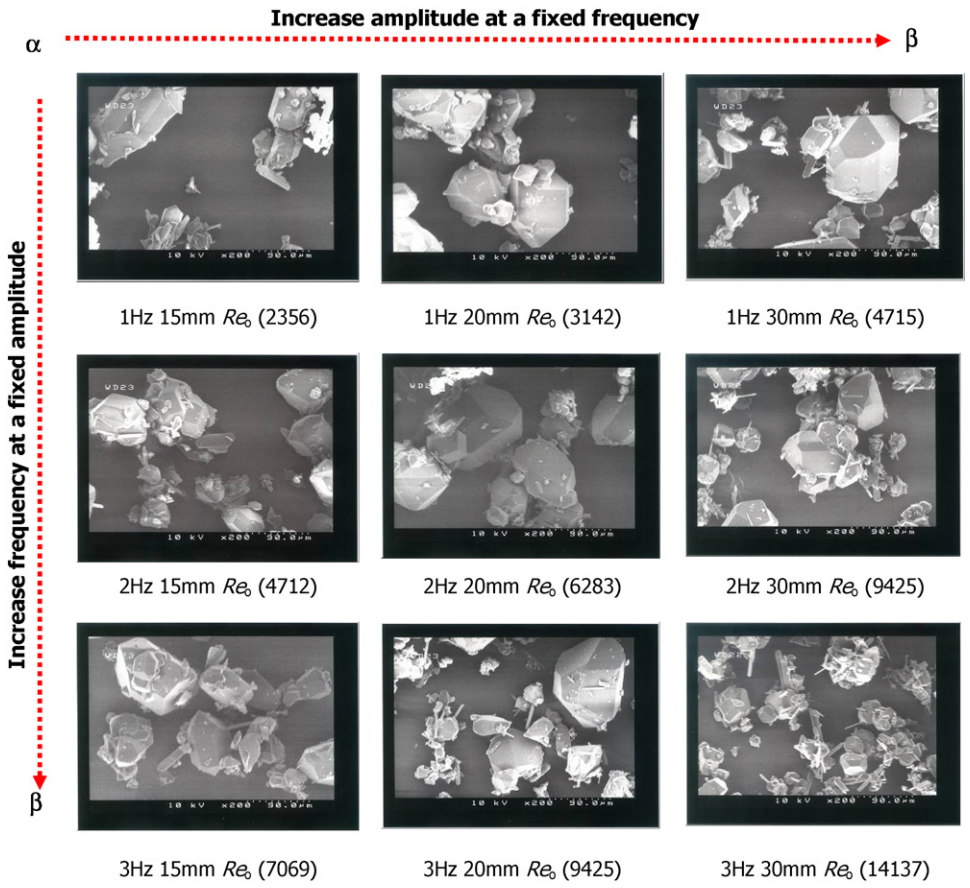

Fig. 7. SEM images of crystals (cooling rate = 0.5 °C min^{-1}, conc. = 30 g L^{-1}).

For α-crystals, crystal size distribution (CSD) was measured using a Malvern Master Sizer, from which mean crystal size can be determined. Fig. 8 shows the averaged crystal size as a function of the oscillatory Reynolds number. The general trend is that the mean crystal size decreased with the increase of the oscillatory Reynolds number. This is in line with the previous studies [42–44]. The decrease of the mean crystal size with the increase of mixing could be attributed to erosion and attrition that were suggested by some researchers [45–48], whom observed breakage and splitting from surfaces of the parent crystals.

3.3. Effect of seeding on polymorph

When a hot and unsaturated solution is cooled, it enters the meta-stable zone and becomes supersaturated. Nucleation takes place within the MSZW via either induction or seeding. The latter is an external means of influencing polymorphism of crystals and is widely used, in fact, almost becomes a pre-requisite procedure in modern pharmaceutical practice. In order to study the effect of seeding on crystal polymorph in the OBC, seeds of either α or β crystals of a mean size of 100 μm [42] were used in experiments for two cooling rates of 0.5 and 2 °C min^{-1} and three concentrations of 30, 40 and 45 g L^{-1} while at the fixed oscillation frequency of 2 Hz and amplitude of 20 mm. A considerable amount of seed is necessary when crystallization condition cannot yield the desired form [49–51]. Based on the previous studies [49,52], 2 g seeds were added into each 0.4 L batch solution just before nucleation takes place. For example, the crystallization temperature at the concentration of 45 g L^{-1} and the cooling rate of 0.5 °C min^{-1} was found to be 60 °C without seeding. For the seeding experiments, the seeds were added when the temperature reached 61 °C, just before its nucleation temperature [53]. This was the experimental protocol used for seeding in this work. Alpha seeds were produced in a beaker in a 30 g L^{-1} solution, which was cooled using ice water and held for 10 min. The crystals were then dried, examined under microscope and confirmed by SEM and XRD. Beta seeds were produced in the similar way in a 48 g L^{-1} solution, which was cooled to 40 °C at 0.5 °C min^{-1} and held for 1 h. Once again, the polymorphism was confirmed by SEM and XRD.

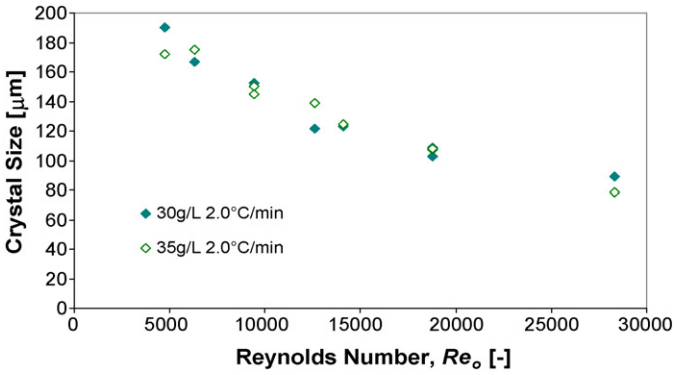

Fig. 8. Mean crystal size of L-glutamic acid vs. oscillatory Reynolds number.

As β crystals are of stable form, operational conditions with fast cooling rates, high solution concentrations and strong mixing allow β crystals to be the dominant polymorph. For meta-stable α crystals, on the other hand, the combination of slower cooling rate, lower solution concentration and gentle mixing would be the operational conditions that favour α crystal formation. The strategy of the seeding experiments was structured so that operating conditions that promoted β crystals were used for seeding α crystals, and

vice versa. In this way, the effect of seeding on crystal morphology is maximised. It should be noted however that seeding with meta-stable α form may reduce meta-stable zone width and induce the growth of the meta-stable crystals but it will not prevent transformation to a more stable form if the system is allowed to run for sufficient time. Equally the stable beta form will never transform to alpha, no matter how much seed is present. Seeding with stable form will promote formation of the stable and transformation of the meta-stable to stable form.

Fig. 9 shows the SEM images of crystals comparing the effects of before and after seeding. At the concentration of 45 g L^{-1}, β crystals were the dominant form (>90%) in the OBC for all cooling rates and mixing conditions. Seeding α crystals at this condition assisted the creation of α-crystals, allowing co-existence of both α and β crystals at the two cooling rates tested. At 40 g L^{-1}, significantly more α crystals were seen for both cooling rates, indicating that the effect of seeding became stronger at the lower solution concentration.

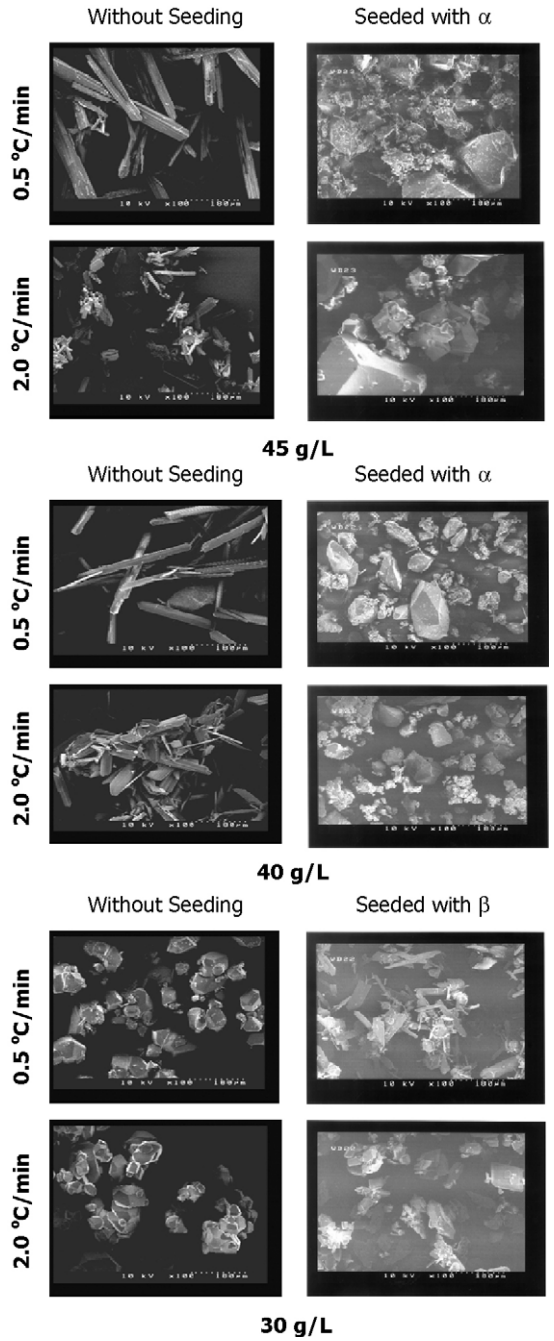

Fig. 9. SEM images of crystals showing the effect of seeding.

Table 2
Effect of seeding on *predominated* polymorph of L-glutamic acid crystals.

	0.5 °C min^{-1}		2.0 °C min^{-1}	
	Before seeding	After seeding	Before seeding	After seeding
30 g L^{-1}	α	β	α	α + β
40 g L^{-1}	β	α + β	β	α + β
45 g L^{-1}	β	α + β	β	α + β

On the other hand, α-form was the leading polymorph at the concentration of 30 g L^{-1} for all cooling rates; seeding β-form led to much more β-crystals within the OBC. As β crystal is the stable form that has the lowest energy state, the effect of seeding β crystals on the change of polymorph was much stronger than the opposite case. Table 2 summarises such effects, showing that seeding assisted either partial or total changes in polymorphism in the crystallization process.

3.4. Effect of baffle materials on MSZW and polymorph

It was reported that the material of a stirrer influenced nucleation in crystallization of L-glutamic acid in a STC [25]. In order to examine whether this effect would exist in the OBC, different material compositions of baffles were tested, e.g. stainless steel (SS) and polyvinylidene difluoride (PVDF), together with various combinations of supporting rods, e.g. SS baffles with PVDF rods with or without threads, in each of the baffle sets. The inclusion of mixed materials was to cover the effect of the spectrum of material selections on this crystallization process. The crystallization experiments were carried out at a fixed solution concentration of 35 g L^{-1}, a fixed oscillation frequency of 2 Hz and amplitude of 20 mm. Table 3 lists the MSZW data together with polymorph for the two cooling rates in the OBC. It seems that the MSZW varied little with the hybrid materials, e.g. SS baffles with PVDF rods; PVDF baffles with threaded SS rods; modified PVDF with PVDF rods, while the changes in MSZW were noticeable for single material arrangement, i.e. either SS or PVDF. Previous studies show that a fourfold increase in crystal count for a stainless steel stirrer than a polyethylene impeller was found in crystallization of $MgSO_4 \cdot 7H_2O$ [54]; a factor of five reduction in the actual nucleation rate constant in ice crystallization was reported when a crystallizer was coated with neoprene and RTV silicone rubber [55]. The probable reason for the reduced nucleation was related to the mechanism of contact nucleation, i.e. the plastic yields on contact with crystal and some of the energy is absorbed by the impeller or coated surfaces, leading to a smaller amount of energy left for action on the growing crystal [54,55]. As energy impact depends on contact angle between solute and surface, contact angle on a rough surface was found smaller than that on a smooth surface, giving a smaller MSZW [25,56]. This would imply that the contact angle, in turn energy absorption, on the stainless steel surface would be smaller than that on the PVDF. To verify the hypothesis, we employed a similar set-up as the previous studies [24,31], i.e. an optical microscopy together with a CCD camera; and measured the contact angles using a testing liquid of a concentration 18 g L^{-1} according to the previous study [24]. These were 78° and 58°, respectively for the PVDF and SS baffles, indicating that the contact angle on the PVDF was much larger than that on the SS surface. The smaller MSZW for the SS baffles is thus confirmed.

Table 3 also summarises the polymorphs of L-glutamic crystals for the materials and their combinations at the two cooling rates. The change of polymorph through the selection of contact materials is clearly seen in the crystallization of L-glutamic acid in the OBC, and α form was noticeably associated with smoother surface.

Table 3
Effect of materials on MSZW and *predominated* morphology (conc. = 35 g L^{-1}, f = 2 Hz and x_o = 20 mm).

	Cooling rate	SS	SS+PVDF	PVDF+ threaded SS	Modified PVDF+PVDF	PVDF
MSZW (°C)	1.0 °C min^{-1}	18	21	21	21	24
Morphology	1.0 °C min^{-1}	β	β	α+β	α+β	α
Morphology	2.0 °C min^{-1}	α+β	α+β	α	α	α
MSZW (°C)	2.0 °C min^{-1}	23	25	24	24	27

Table 4
Predominated crystal morphology for different final temperatures (conc. = 35 g L^{-1}, f = 2 Hz and x_o = 20 mm).

b	Final temperature				
	5 °C	10 °C	20 °C	35 °C	40 °C
1.0 °C min^{-1}	α	α	α	α + β	β
2.0 °C min^{-1}	α	α	α	α + β	α + β

3.5. Effect of final temperature on polymorph

So far in this work, a final temperature of 10 °C was used in the experiments. In order to examine the effect of final temperature on crystal polymorph, the following sets of tests were carried out by varying the final temperature from 5 to 40 °C at a fixed solution concentration of 35 g L^{-1} and at two cooling rates 1 and 2 °C min^{-1}, respectively while keeping the rest conditions, such as mixing intensity, the starting temperature, the nucleation temperature, unchanged. At each cooling rate, the slope of cooling or temperature profile was also the same, the only variable was the end point or temperature. Table 4 summarises crystal polymorphism for various final temperatures. As the solubility of α crystals is always higher than that of β form [31], the dissolution of α crystals would be more favourite at higher temperature, promoting the transformation from α to β form. Ono et al. [57] also reported that the dissolution rate of α-form L-glutamic acid was fast at 50 °C, and the higher the final temperature, the higher the transformation rate. The final temperature would also affect supersaturation achieved in the system, hence influences the final crystal form. The data in Table 4 clearly demonstrate the transformation of meta-stable α to stable β form when the final temperature was 35 °C or higher that is closer to its nucleation temperature. We also see that under the operation conditions, the lower the final temperature, the more the α crystals. As a result, controlling final temperature in crystallization of L-glutamic acid is another parameter influencing crystal polymorphism.

4. Conclusions

The results from this work show that the MSZW is decreased with the increase of mixing; such an effect was stronger for higher cooling rates and the meta-stable α crystals were transformed into the stable β crystals with enhanced mixing. Seeding α crystals in experimental conditions with predominantly β form caused the formation of α crystals allowing the co-existence of both forms; while seeding β crystals in conditions that favour α form led to much intensified polymorph transformation.

Our results also show that the materials of baffles affected the crystal polymorph. The smoother surface exhibited larger MSZW and favoured for the meta-stable crystals, while the rougher surface had smaller MSZW with the stable crystals dominating. The effect of final cooling temperature on polymorphism is that meta-stable crystals gradually changed into the stable form when it was closer to its crystallization temperature. The outcomes of this study suggest that by controlling process parameters desirable crystal polymorph can be obtained.

Nomenclature

D	column diameter (m)
f	oscillation frequency (Hz)
Re_o	the oscillatory Reynolds number
St	the Strouhal number
T_{sat}	saturation temperature (°C)
T_{cry}	crystallization temperature (°C)
x_o	oscillation amplitude (m)
μ	fluid viscosity (kg m^{-1} s^{-1})
ρ	fluid density (kg m^{-3})

Acknowledgement

AL wishes to thank for the Heriot-Watt University for the Scholarship.

References

[1] J. Ulrich, C. Strege, Some aspects of the importance of metastable zone width and nucleation in industrial crystallisers, Journal of Crystal Growth 237–239 (2002) 2130–2135.
[2] A.W. Nienow, M.F. Edwards, N. Harnby, Mixing in the Process Industries, 2nd edition, Butterworth-Heinemann, 1997.
[3] J.R. Couper, W.R. Penney, J.R. Fair, Chemical Process Equipment: Selection and Design, Gulf Professional Publishing, 2004, pp. 776–779.
[4] E.B. Nauman, Chemical Reactor Design, Optimization and Scaleup, McGraw-Hill Professional, 2002, pp. 600–605.
[5] G.W. Smith, L.L. Tavlarides, J. Placek, Turbulent flow in stirred tanks: scale-up computations for vessel hydrodynamics, Chemical Engineering Communication 93 (1990) 49–73.
[6] M. Kraume, P. Zehner, Concept for scale-up of solids suspension in stirred tanks, Canadian Journal of Chemical Engineering 80 (4) (2002) 674–681.
[7] D. Thoenes, Chemical Reactor Development: From Laboratory Synthesis to Industrial Production, Springer, 1994, pp. 347–354.
[8] F.W.J.M.M. Hoeks, L.A. Boon, F. Studer, M.O. Wolff, F. van der Schot, P. Vrabel, R.G.J.M. van der Lans, W. Bujalski, A. Manelius, G. Blomsten, S. Hjorth, G. Prada, K.C.A.M. Luyben, A.W. Nienow, Scale up of stirring as foam disruption (SAFD) to industrial scale, Journal of Industrial Microbiology and Biotechnology 30 (2) (2003) 118–128.
[9] V.B. Shukla, U. Parasu Veera, P.R. Kulkarni, A.B. Pandit, Scale-up of biotransformation process in stirred tank reactor using dual impeller bioreactor, Biochemical Engineering Journal 8 (1) (2001) 19–29.
[10] M.J. Whitton, A.W. Nienow, Scale up correlations for gas holdup and mass transfer coefficients in stirred tank reactors, in: 3rd International Conference on Bioreactor and Bioprocess Fluid Dynamics, Mechanical Engineering Publications Ltd., Cambridge, UK, 1993.
[11] J.K. Kim, C.K. Kim, J. Kawasaki, A scale up of stirred tank contactors for the liquid membrane permeation of hydrocarbons, Separation Science and Technology 36 (16) (2001) 3585–3598.
[12] U. Parasu Veera, A.W. Patwardhan, J.B. Joshi, Measurement of gas hold-up profiles in stirred tank reactors by Gamma ray attenuation technique, Transactions of the Institute of Chemical Engineers 79 (A6) (2001) 684–688.
[13] J.J. Evangelista, S. Katz, R. Shinnar, Scale-up criteria for stirred tank reactors, American Institute of Chemical Engineers Journal 15 (6) (2004) 843–853.

[14] M. Li, G. White, D. Wilkinson, K.J. Roberts, Scale up study of retreat curve impeller stirred tanks using LDA measurements and CFD simulation, The Chemical Engineering Journal 108 (1–2) (2005) 81–90.
[15] C.D. Rielly, A.J. Marguis, A particle's eye view of crystallizer fluid mechanics, Chemical Engineering Science 56 (2001) 2475–2493.
[16] L. Xie, C.D. Rielly, W. Eagles, G. Özcan-Taşkin, Dispersion of nano-particle clusters using mixed flow and high shear impellers in stirred tanks, Chemical Engineering Research and Design 85 (A5) (2007) 676–684.
[17] L. Xie, C.D. Rielly, G. Özcan-Taşkin, Break-up of Nano-particle Agglomerates by Hydrodynamically Limited Processes, BHR Group 2007 Industrial Processes for Nano and Micro Products, 2007.
[18] X. Ni, M.R. Mackley, A.P. Harvey, P. Stonestreet, M.H.I. Baird, N.V. Rama Rao, Mixing through oscillations and pulsations—a guide to achieving process enhancements in the chemical and process industries, Transactions of the Institute of Chemical Engineers 81 (A) (2003) 373–383.
[19] X. Ni, H. Jian, A numerical study on the scale up behaviour in oscillatory baffled columns, Chemical Engineering Research and Design 83 (2005) 1163–1170.
[20] X. Ni, A. Liao, Effects of cooling rate and solution concentration on solution crystallisation of L-glutamic acid in an oscillatory baffled crystalliser, Crystal Growth and Design 8 (2008) 2875–2881.
[21] X. Ni, P. Gough, On the discussion of the dimensionless groups governing oscillatory flow in a baffled tube, Chemical Engineering Science 52 (1997) 3209–3212.
[22] J. Nyvlt, Kinetics of nucleation in solution, Journal of Crystal Growth 3 (4) (1968) 377–383.
[23] J. Nyvlt, R. Rychly, J. Gottfried, J. Wurzelova, Metastable zone-width of some aqueous solution, Journal of Crystal Growth 6 (1970) 151–162.
[24] J.K. Liang, Process Scale Dependence of Batch Crystallisation L-glutamic Acid from Aqueous Solution in Relation to Reactor Internals Reactant Mixing and Process Conditions, Heriot-Watt University, Edinburgh, 2002.
[25] K.W.G. Liang, D. Wikinson, L.J. Ford, K.J. Roberts, W.M.L. Wood, An examination into the effect of stirrer material and agitation rate on the nucleation of L-glutamic acid batch crystallized from supersaturated aqueous solutions, Crystal Growth and Design 4 (5) (2004) 1039–1044.
[26] L.A. Smith, K.J. Roberts, D. Machin, G. McLeod, An examination of the solution phase and nucleation properties of sodium, potassium and rubidium dodecyl sulphates, Journal of Crystal Growth 226 (2001) 158–167.
[27] M. Karel, J. Nyvlt, A. Chianese, Crystallization of pentaerythritol. I. Solubility, density and metastable zone width, Collection of Czech Chemical Communications 59 (1994) 1261–1269.
[28] J.H. Lee, J.H. Kim, I.H. Zhu, X.B. Zhan, J.W. Lee, D.H. Shin, S.K. Kim, Optimisation of conditions for the production of pullulan and high molecular weight pullulan by *Aureobasidium pullulans*, Biotechnology Letters 23 (2001) 817–820.
[29] H. Gron, P. Mougin, A. Thomas, G. White, D. Wilkinson, Dynamic in-process examination of particle size and crystallographic form under defined conditions of reactant supersaturation as associated with the batch crystallisation of monosodium glutamate from aqueous solution, Industrial and Engineering Chemical Research 42 (2003) 4888–4898.
[30] J. Garside, A. Mersmann, J. Nyvlt, Measurement of Crystal Growth and Nucleation Rate, IChemE, UK, 2002.
[31] Y. Sakata, Studies on the polymorphism of L-glutamic acid part. I: effect of coexisting substance on polymorphic crystallization, Agricultural and Biological Chemistry 25 (11) (1961) 835–837.
[32] J.W. Mullin, Crystallisation, Butterworth-Heinnemann, 1993.
[33] A.S. Meyerson, Handbook of Industrial Crystallization, B.-H.S.i.C. Engineering, London, 1993.
[34] A.R. Gerson, K.J. Roberts, J.N. Sherwood, An instrument for the examination of nucleation form solution and its application to the study of precipitation from diesel fuels and solution of n-alkanes, Power Technology 65 (1991) 243–249.
[35] A.I. Kitaigorodsky, Order and Disorder in the World of Atoms, Mir Publishers, Moscow, 1980.
[36] P. Bennema, G.H. Gilmer, in: P. Hartman (Ed.), Crystal Growth: An Introduction, North-Holland, Amsterdam, 1973.
[37] D.L. Klug, in: A.S. Meyerson (Ed.), Handbook of Industrial Crystallisation, Butterworths, New York, 1993.
[38] I. Weissbuch, L. Leiserowitz, M. Lahav, in: A. Mersmann (Ed.), Crystallisation Technology Handbook, Marcel Dekker, New York, 1995.
[39] X. Ni, A. Valentine, A. Liao, S.B.C. Sermage, G.B. Thomson, K.J. Roberts, On the crystal polymorphic forms of L-glutamic acid following temperature programmed crystallisation in a batch oscillatory baffled crystalliser, Journal of Crystal Growth and Design 4 (2004) 1129–1135.
[40] Y.H.K. Cheon, S.-H. Kim, A study on crystallization kinetics of pentaerythritol in a batch cooling crystallizer, Chemical Engineering Science 60 (2005) 4791–4802.
[41] M. Kitamura, Polymorphism in the crystallisation of L-glutamic acid, Journal of Crystal Growth 96 (1989) 541–546.
[42] L.G. Bauer, R.W. Rousseau, W.L. McCabe, Influence of crystal size on the rate of contact nucleation in stirred-tank crystallizers, American Institute of Chemical Engineers Journal 20 (4) (1974) 653–659.
[43] I. Liszi, M. Hasznos-Nezdei, B. Farkas, Effect of mixing on primary nucleation, Hungarian Journal of Industrial Chemistry 25 (1997) 181–184.
[44] B.Y. Shekunov, J. Baldyga, P. York, Particle formation by mixing with supercritical antisolvent at high Reynolds numbers, Chemical Engineering Science 56 (2001) 2421–2433.
[45] G. Gahn, J. Krey, A. Mersmann, The effect of impact energy and the shape of crystals on their attritions rate, Journal of Crystal Growth 166 (1996) 1058–1063.
[46] P.A. Shamlou, A.G. Jones, K. Djamarni, Hydrodynamics of secondary nucleation in suspension crystallisation, Chemical Engineering Science 45 (5) (1990) 1405–1416.
[47] A. Chianese, F.D. Berardino, A.G. Jones, On the effect of secondary nucleation on the crystal size distribution from a seeded batch crystallizer, Chemical Engineering Science 48 (3) (1993) 551–560.
[48] M. Liiri, T. Koiranen, J. Aittamaa, Secondary nucleation due to crystal-impeller and crystal-vessel collisions by population balances in CFD-modelling, Journal of Crystal Growth 237–239 (2002) 2188–2193.
[49] D. Jagadesh, N. Kubota, M. Yokota, N. Doki, A. Sato, Seeding effect on batch crystallization of potassium sulfate under natural cooling mode and a simple design method of crystallizer, Journal of Chemical Engineering of Japan 32 (4) (1999) 514–520.
[50] N. Kubota, N. Doki, M. Yokota, D. Jagadesh, Seeding effect on product crystal size in batch crystallization, Journal of Chemical Engineering of Japan 35 (11) (2002) 1063–1071.
[51] S.H. Chung, D.L. Ma, R.D. Braatz, Optimal seeding in batch crystallization, The Canadian Journal of Chemical Engineering 77 (1999) 590–596.
[52] N.Y.M. Doki, K. Kido, S. asaki, N. Kubota, Reliable and selective crystallization of the metastable a-form glycine by seeding, Crystal Growth and Design 4 (1) (2004) 103–107.
[53] W. Beckmann, Seeding the desired polymorph: background, possibilities, limitations, and case studies, Organic Process Research & Development 4 (2000) 372–383.
[54] B.C. Shah, W.L. McCabe, R.W. Rousseau, Polyethylene vs. stainless steel impellers for crystallisation processes, American Institute of Chemical Engineers Journal 19 (1) (1973) 194–1194.
[55] T.W. Evans, G. Margolis, A.F. Sarofim, Mechanisms of secondary nucleation in agitated crystallisers, American Institute of Chemical Engineers Journal 20 (5) (1974) 950–958.
[56] E. Curcio, E. Fontananova, G. Di Profio, E. Drioli, Influence of the structural properties of poly(vinylidene fluoride) membranes on the heterogeneous nucleation rate of protein crystals, Journal of Physical Chemistry B 110 (2006) 12438–12445.
[57] T. Ono, H.J.M. Kramer, J.H. ter Horst, P.J. Jansens, Process modelling of the polymorphic transformation of L-glutamic acid, Crystal Growth and Design 4 (6) (2004) 1161–1167.